RESEARCH ARTICLE

Cross-kingdom RNAi induced by a beneficial endophytic fungus to its host requires transitivity and amplification of silencing signals

L. M. Kellari[1,2], A. Dalakouras[3], O. Tsiouri[1], P. Vletsos[1], A. Katsaouni[1], V. V. Uslu[4,5] & K. K. Papadopoulou[1,2] (iD)

1 Department of Biochemistry and Biotechnology, Laboratory of Plant and Environmental Biotechnology, University of Thessaly, Larissa, Greece
2 Averofeio Agri-Food Technological Park of Thessaly, University of Thessaly, Larissa, Greece
3 Hellenic Agricultural Organization Demeter, Institute of Industrial and Forage Crops, Larissa, Greece
4 RLP AgroScience GmbH, Neustadt an der Weinstrasse, Germany
5 Center for Organismal Studies, Heidelberg University, Heidelberg, Germany

ABSTRACT

- Cross-kingdom transfer of small RNA (sRNA) molecules has been identified as a means of communication between plants and interacting microorganisms, but the mechanistic details of this sRNA-based interaction remain elusive. We have previously shown that the beneficial root-colonizing fungus *Fusarium solani* strain K (FsK) translocates sRNAs to its host, *Nicotiana benthamiana* (Nb), leading to systemic silencing of a reporter gene.
- Here, we investigated the mechanistic details of the endophyte-induced systemic silencing using an RNAi sensor system. We inoculated three Nb GFP expressing lines with conidia of an FsK transformant containing a transgene that targets host GFP (FsK-hpGF). The efficiency of silencing mediated by FsK-hpGF was monitored both phenotypically under ultraviolet light as well as quantitatively by RT-qPCR. sRNA sequencing was performed to evaluate the production of sRNAs targeting host GFP. Finally, bisulfite sequencing was used to assess plant GFP methylation levels.
- We show that the translocated fungal sRNAs induced production of secondary sRNAs, mainly of 22–24-nt in size, with the conspicuous absence of 21-nt sRNAs. Importantly, systemic silencing could not be induced in an *RNA-DEPENDENT RNA POLYMERASE 6* (*RDR6*) CRISPR/Cas knockout background, nor in an intron-containing target gene.
- Overall, our data show that endophyte-induced silencing in the host requires RDR6-mediated transitivity and amplification of silencing signals. Despite being based on an artificial RNAi sensor system, our observations may reflect a more generalized and so far unexplored facet of cross-kingdom RNAi, with RDR6-based transitivity influencing the way symbionts and pathogens elicit systemic phenotypes in their host plants.

INTRODUCTION

RNA interference (RNAi) is a conserved mechanism of gene regulation in eukaryotes, where double stranded RNAs (dsRNAs) are cleaved by DICER-LIKE endonucleases (DCLs) into small RNAs (sRNAs) that are loaded on ARGONAUTE proteins (AGOs) to mediate mRNA cleavage and/or translational arrest and/or epigenetic modifications (Vaucheret & Voinnet 2024). In flowering plants, with the exception of DCL1 that uses as substrates stem loop hairpin RNAs and is involved in micro RNA (miRNA) biogenesis (Reinhart *et al.* 2002; Zhan & Meyers 2023), three DCLs act redundantly and compete for the same dsRNA substrate (Henderson *et al.* 2006; Zapletal *et al.* 2023). DCL4 generates 21-nt sRNAs that are loaded on AGO1 and cleave complementary mRNAs in the cytoplasm, in a process termed post-transcriptional gene silencing (PTGS) (Hamilton & Baulcombe 1999; Zhan &

Meyers 2023). DCL3 cleaves dsRNAs to 24-nt sRNAs that are loaded on AGO4 and recognize cognate DNA (or its nascent transcript) in the nucleus (Chan *et al.* 2004; Wang *et al.* 2023), recruiting de novo methyltransferase DOMAINS REARRANGED 2 (DRM2) to methylate cytosine residues in all sequence contexts (CG, CHG, CHH) (Cao *et al.* 2003; Leichter *et al.* 2022) in a process termed RNA-directed DNA methylation (RdDM) (Wassenegger *et al.* 1994; Wassenegger & Dalakouras 2021). Finally, DCL2 generates 22-nt sRNAs that are loaded to AGO1 and recruit RNA-DEPENDENT RNA POLYMERASE 6 (RDR6) to the very 3′ end of the targeted transcript (Mlotshwa *et al.* 2008; Chen *et al.* 2010). The activity of RDR6 culminates in the occurrence of secondary dsRNA and sRNAs that amplify the sRNA pool and reinforce RNAi, a mechanism named transitivity (Dalmay *et al.* 2000; de Felippes & Waterhouse 2020). Importantly, plant sRNAs are not cell-restricted but may move through plasmodesmata to neighbouring cells,

and through the vasculature to distant parts of the plant, establishing systemic RNAi (Voinnet & Baulcombe 1997; Devers et al. 2023).

A growing body of evidence suggests that plants interact with microbes, in a bi-directional cross-kingdom RNAi manner (Cai et al. 2023; Cheng et al. 2023). Indeed, plants defend against pathogenic fungi by sending sRNAs that target fungal pathogenicity genes: cotton to Verticillium dahliae (Zhang et al. 2016), Arabidopsis to Botrytis cinerea (Cai et al. 2018), and wheat to Fusarium graminearum (Jiao & Peng 2018). In reverse, pathogenic fungi fight back and translocate sRNAs to the plants to mitigate their defence: B. cinerea to tomato (Weiberg et al. 2013), V. dahliae to Arabidopsis (Wang et al. 2016), and Puccinia striiformis to wheat (Wang et al. 2017). However, it is not only pathogenic fungi that communicate in such a sRNA-based manner with their hosts; beneficial fungi also do it. In silico studies coupled with sRNA and transcriptome analysis had suggested that the beneficial arbuscular mycorrhizal fungus, Rhizophagus irregularis, produces sRNAs predicted to target more than 200 transcripts in the host plant Medicago truncatula (Silvestri et al. 2019), and similar conclusions were drawn for the interaction between the beneficial root endophyte Serendipita indica and its host Brachypodium distachyon (Secic et al. 2021). More recently, the ectomycorrhizal fungus Pisolithus microcarpus was shown to deliver sRNAs to its host Eucalyptus grandis to trigger RNAi and stabilize symbiotic interactions (Wong-Bajracharya et al. 2022). In a biotechnological approach termed 'microbe-induced gene silencing' (MIGS), the rhizospheric beneficial fungus Trichoderma harzianum was engineered to deliver sRNAs designed to target the soilborne pathogenic fungi V. dahliae and F. oxysporum in cotton and rice plants (Wen et al. 2023). How these sRNAs are transferred is not clear, but evidence shows that plants use extracellular vesicles (EVs) to deliver sRNAs to fungal pathogens, as is the case of Arabidopsis and B. cinerea (Cai et al. 2018). Similarly, B. cinerea uses the same mechanism to send sRNAs to Arabidopsis that enter the plant mainly through clathrin-mediated endocytosis (He et al. 2021; Cai et al. 2023). However, other reports suggest that sRNAs located outside of extracellular vesicles (not inside them) are the primary mediators of cross-kingdom RNAi phenomena (Zand Karimi et al. 2022).

Fusarium solani strain K (FsK) is a non-pathogenic strain of F. solani with an endophytic lifestyle (Kavroulakis et al. 2007; Skiada et al. 2020). We have previously shown that FsK encodes 2 DCL, 2 AGO and 4 RDR genes (Dalakouras et al. 2023). We have also constructed a sensor system using an FsK transgenic strain, which harboured both a GFP expressing part as well as a hairpin RNA targeting only the upstream 322 bp part of the 792 bp GFP, namely FsK-hpGF (Fig. 1A). We showed that, in the fungal hyphae, the hairpin hpGF, was processed by fungal DCLs predominantly into 21-nt sRNAs that mediated mRNA degradation but not transitivity nor DNA methylation of a GFP reporter gene; notably, the enzyme responsible for the processing of hpRNA/dsRNA to siRNAs in fungal hyphae is most probably FsKDCL2, rather than FsKDCL1, the latter is mainly involved in meiotic silencing by the unpaired DNA (MSUD) pathway (Dalakouras et al. 2023). Importantly, when FsK-hpGF, which has a root-restricted growth in N. benthamiana, colonized its host stably expressing a GFP reporter gene (Nb-GFP16C), this triggered systemic RNA silencing of the host GFP. In the present study, we explore the mechanistic details of FsK-induced silencing in its host N. benthamiana. Our hypothesis was that the systemic silencing is unlikely to be triggered by the translocated primary fungal sRNAs in colonized roots. On the contrary, an amplification of RNAi signals would be required through the generation of secondary sRNAs in the host. By using a series of different RNAi sensor reporter genes and a genetic approach (intronless and intron-containing in wild type and rdr6 knockout background plant lines), we were able to confirm this hypothesis.

MATERIAL AND METHODS

Plant colonization with FsK

Nb-GFP16C, Nb-GFPendo, and Nb-GFP16C/rdr6 seeds were surface-sterilized for 10 min using 10% (v/v) NaOCl solution and washed six times with sterile deionized water. Seeds were kept in deionized water in the dark for 2 h and subsequently planted on sterile sand substrate. Seedlings were repotted 10 days after germination in magenta pots containing sterile sand: vermiculite substrate (3:1). Each pot containing one plant is considered as one biological replicate. Pots were alternatively watered with full strength Hoagland medium or dH_2O. Plants were grown in a growth chamber with a 16 h light/8 h dark photoperiod at 25 °C. FsK-hpGF was cultured for 5 days in potato dextrose broth (25 °C, 160 rpm). Conidia suspension was collected after sieving mycelium fragments through sterile double layered cheesecloth. Conidia were recovered from the filtrate with centrifugation at 5500 rpm, counted using a haemocytometer and suspended in the appropriate amount of 0.85% (w/v) NaCl to achieve the desired concentration. For the systemic RNAi test, Nb-GFP16C plants were separated into four categories each represented by 15 plants: Mock-inoculated controls and inoculated with FsK-hpGF conidia at different amounts (10^2, 10^3, 10^4). Nb-GFPendo were separated into two categories each represented by 14 plants: Mock-inoculated controls and inoculated with 10^3 FsK-hpGF conidia. Nb-GFP16C/rdr6 plants were subdivided into two categories each represented by 10 plants: Mock-inoculated controls and inoculated with 10^3 FsK-hpGF conidia. Control plants inoculated with non-transformed FsK were also included. Inoculation was performed at the two true leaf stage. Plants were harvested at 9 wpi as follows. For the roots, the whole root system was sampled, whereas for the leaves only the tissue with the RNAi phenotype was harvested. For plants with no RNAi phenotype, whole leaf tissue was sampled.

Reverse transcriptase quantitative polymerase chain reaction (RT-qPCR)

Total RNA from plant material was isolated with TRIzol™ reagent according to the manufacturer's instructions (www.thermofisher.com). The DNase I-treated RNA isolated from plant tissues was quantified using a Qubit® 2.0 Fluorometer (www.thermofisher.com). The DNA-free RNA was diluted to 10 ng μl⁻¹ and subsequently used for RT-qPCR using Luna® Universal One-Step RT-qPCR Kit (www.neb.com) following manufacturer's instructions. Total volume of the reaction was
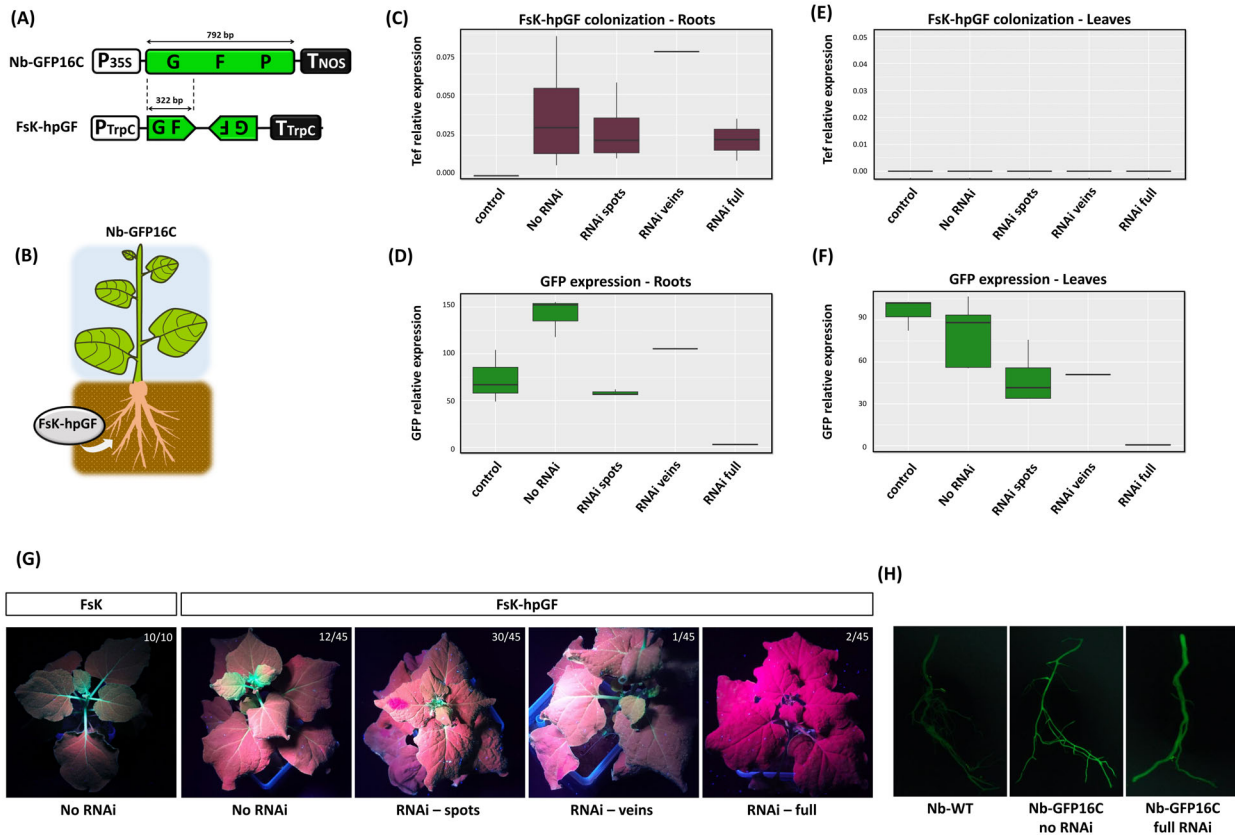
Fig. 1. Fsk hpGF colonization of Nb-GFP16C plants. (A) Schematic representation of the *GFP* transgene present in Nb-GFP16C line and the hpGF construct of FsK. P35S: Cauliflower mosaic virus *35S* promoter; GFP: Full-length (792 bp) green fluorescent protein (*mGFP-ER* version); TNOS: Terminator for the *NOPALINE SYNTHASE* (*NOS*) gene, PTrpC promoter from *Aspergillus nidulans trpC* gene; GF: 322 Bp fragment of the *GFP*; TTrpC: Terminator from *Aspergillus nidulans trpC* gene. (B) Schematic overview of the colonization assay. (C) RT-qPCR for the estimation of fungal colonization levels (*Tef* gene) in roots of the Nb-GFP16C plants at 9 wpi. Expression levels are normalized to the *Nb Actin* (*Act*) gene. Data are categorized per silencing phenotype, each represented by different biological replicates (n), with all samples run in two technical replicates (Control: N = 3, No RNAi: N = 4, RNAi spots: N = 4, RNAi veins: N = 1, RNAi full: N = 2). (D) RT-qPCR for the estimation of *gfp* mRNA downregulation in roots of the systemically silenced plants at 9 wpi. Expression levels are normalized to the *Nb Act* gene. Data are categorized per silencing phenotype, each represented by different biological replicates (n), with all samples run in two technical replicates (Control: N = 3, No RNAi: N = 4, RNAi spots: N = 4, RNAi veins: N = 1, RNAi full: N = 2). (E) RT-qPCR for the estimation of fungal colonization levels (*Tef* gene) in leaves of the Nb-GFP16C plants at 9 wpi. Expression levels are normalized to the *Nb Act* gene. Data are categorized per silencing phenotype, each represented by different biological replicates (n), with all samples run in two technical replicates (Control: N = 3, No RNAi: N = 4, RNAi spots: N = 4, RNAi veins: N = 1, RNAi full: N = 2). (F) RT-qPCR for the estimation of *gfp* mRNA downregulation in leaves of the systemically silenced plants at 9 wpi. Expression levels are normalized to the *Nb Act* gene. Data are categorized per silencing phenotype, each represented by different biological replicates (n), with all samples run in two technical replicates (Control: N = 3, No RNAi: N = 4, RNAi spots: N = 4, RNAi veins: N = 1, RNAi full: N = 2). (G) Systemic silencing phenotypes under ultraviolet light at 6–7 wpi (in total 45 FsK-hpGF-inoculated Nb-GFP16C plants were studied). Control plants inoculated with non-transformed wild type FsK show no RNAi phenotype (H) Stereoscopic observation of GFP fluorescence in roots of non-colonized versus fully silenced Nb-GFP16C plants at 9 wpi. Nb wild type (Nb-WT) was used as a negative control of root autofluorescence.

reduced to 10 μl, and cycling conditions consisted of incubation at 55 °C for 10 min for reverse transcription, 95 °C for 1 min, followed by 30 cycles of 95 °C for 10 s and 60 °C for 30 s, and a melting curve to check specificity of the products. The relative expression of *gfp* (133 bp amplicon) and *Tef* (120 bp amplicon) genes was calculated for two technical replicates per sample and the *N. benthamiana Act* (169 bp amplicon) gene was used as an internal control. All primers used are listed in Table S1. Analysis was carried out using the ΔCT method (Livak & Schmittgen 2001). Visualization of data was done in R studio using the ggplot2 package. Statistical data analysis was done using Student's two-tailed homoscedastic *t*-test.

Bisulfite sequencing

Genomic DNA from the plant (100 ng) was isolated using the CTAB DNA extraction method. Bisulfite sequencing analysis was performed using the EZ DNA Methylation-Gold Kit (www.zymoresearch.com) according to the manufacturer's instructions and as previously described (Dalakouras et al. 2016a). To analyse a 206 bp "G" fragment in both Nb-GFP16C and Nb-GFPendo, the primers BisG-F and BisG-R were used. To analyse a 356 bp "P" fragment in both Nb-GFP16C and Nb-GFPendo, the primers BisP-F and BisP-R were used. The occurring amplicons were cloned into pGEM®-T Easy Vector (www.promega.com), and for each

analysis five clones were subjected to Sanger sequencing. The data were analysed using CyMATE software (Hetzl *et al.* 2007).

Small RNA sequencing

For small RNA sequencing the RNA fraction below 150 nt was isolated using the NucleoSpin miRNA kit (www.mn-net.com) according to the manufacturer's instructions. Sequencing of small RNAs from the plant small RNA fraction was performed by GenXPro (https://genxpro.net/). Small RNA libraries were prepared using the TrueQuant small RNA Seq Kit (GenXPro) according to the manual of the manufacturer. In brief, adapters including TrueQuant molecular identifiers were ligated to the small RNAs followed by reverse transcription and PCR. Sequencing was performed on an Illumina NextSeq500 instrument with 1×75 bps. Unprocessed sequencing reads were adapter-trimmed and quality-trimmed using Cutadapt (Martin 2011). Deduplication based on UMIs (Unique Molecular Identifier) was performed using in-house tools. FastQC was used to assess the quality of sequencing reads. Processed sequencing reads were mapped with a reference genome using Bowtie2 (Langmead & Salzberg 2012). Quantification of mapped reads to each transcript was performed using HTSeq (Anders *et al.* 2014). MultiQC (Ewels *et al.* 2016) was used to create a single report visualizing output from multiple tools across many samples, enabling global trends and biases to be quickly identified. For the visualization of sRNA reads aligned to the reference sequence (GFP), Tablet software was used (Milne *et al.* 2013). To detect 21-nt sRNAs reads mapping to the host genome, selection of 21-28-nt reads was performed with cutadapt v. 2.8 (Martin 2011). The *N. benthamiana* v. 2.6.1 transcriptome downloaded from solgenomics.net (Fernandez-Pozo *et al.* 2015) was used to map the 21–28 nt reads of each sample using bowtie v. 1.2.3 (Langmead *et al.* 2009) with parameters than can be described in the following github repository (https://github.com/olgatsiouri1996/siRNA-mapped-to-Niben-length-distribution). To detect conserved *N. benthamiana* 21-nt miRNAs in our 21-nt sRNA dataset, the four most abundant were selected (Baksa *et al.* 2015). Mapping of the dataset's reads to each of the miRNAs sequence was done with bowtie v. 1.2.3 (Langmead *et al.* 2009) with parameters–v 0 –norc–best–strata–m 1–l 21, in order to report only the best hit per read (–best –strata–m 1), search only the forward orientation of reads (–norc), with a seed length of 21 (−l 21) and require that the reads and the sequence have 100% similarity in all 21 nt (−v 0). Fastq and bam files used in this analysis can be found at https://doi.org/10.5281/zenodo.10044132. Stacked bar charts showing siRNA length distribution were made in R studio using the package ggplot2.

GFP fluorescence monitoring

Green fluorescence of Nb-GFP16C, Nb-GFPendo, and Nb-GFP16C/rdr6 upper part was monitored once a week for 9 weeks post-inoculation using a handheld Black-Ray B-100AP High Intensity UV Lamp (UVP). Pictures were taken with a Xiaomi (2109119DG camera model) phone. Root fluorescence was monitored with a Leica MZ 10 F stereoscope with a GFP filter. Photographs were taken with an Olympus digital camera.

RESULTS AND DISCUSSION

FsK triggers RNAi and transitivity of an intronless gene in both root and leaves

FsK in *N. benthamiana* colonizes only the root, but silencing spreads systemically throughout the whole plant (Dalakouras *et al.* 2023). Based on these results, it was not clear whether the fungal (primary) GF sRNAs could alone be accountable for this spreading of RNAi or whether a transitivity-based amplification of RNAi takes place, and if so, whether transitivity is initiated already at the root tissues. To address these issues, we inoculated *N. benthamiana* plant line, Nb-GFP16C, with the transgenic hairpin expressing strain FsK-hpGF (Fig. 1A,B) and verified by RT-qPCR analysis that, indeed, FsK-hpGF colonized only the root but not the aerial parts of the plant (Fig. 1C,E). Already at 2 weeks post-inoculation (wpi), under ultraviolet (UV) light we could observe systemic silencing phenotypes in the leaf tissues, ranging from silencing spots to vein-restricted and full silencing (Fig. 1G). Of note, colonization of Nb-GFP plants with non-transformed FsK failed to trigger any visible RNAi phenotype (Fig. 1G) even after 10 wpi, corroborating previous observations (Dalakouras *et al.* 2023) and suggesting that it is not the mere presence of the endophyte, but the specific RNAi molecules it expresses that are responsible for the induction of RNAi phenotypes in its host.

To further investigate the silencing phenotype in the root tissues, we first recorded, by fluorescent microscopy, whether the roots of the systemically silenced plants were also silenced (Fig. 1H). Yet, we were not able to arrive at any safe conclusions due to the strong root autofluorescence of the *N. benthamiana* plants (Fig. 1H). To tackle this issue, we used an RT-qPCR approach for detecting expression levels of the plant *gfp* transgene, both in the leaf and root tissues of the silenced plants. Indeed, reduced gene expression was revealed not only in the leaf tissues analysed but also in the root tissues of the systemically fully silenced plants (Fig. 1D,F). We then investigated in detail the putative effect of the inoculum concentration on the appearance of the silencing phenotypes to determine whether a threshold of fungal biomass is needed intraradically for the silencing phenotypes to appear. We inoculated the plants with a range of 10^2–10^4 conidia per seedling by root drenching. Notably, the efficiency of silencing phenotypes did not seem to correlate with the FsK-hpGF inoculation titre (Figure S1).

Having established the systemic silencing phenotype in our sensor plant–endophyte system, we then proceeded with sRNA sequencing analysis in both root and leaf tissues of the systemically fully-silenced plants. According to our hypothesis, we were expecting and wanted to assess the population of (a) the primary sRNAs, that is, the sRNAs deriving from the fungus and corresponding to the partial *gfp* gene (1–322 bp) that is harboured by the fungus (GF sRNAs), and (b) the secondary sRNAs, that is, the sRNAs deriving in the plant by the activity of RDR6, that is, GF and P sRNAs, corresponding to the relative regions of the *GFP* gene. Our data analysis revealed the accumulation of both GF (1–322 bp) and P (323–792 bp) sRNAs, demonstrating that RDR6-based transitivity was initiated and secondary sRNAs were detected (Fig. 2A). The transitive sRNA pattern was identical in both root and leaf tissues (Fig. 2A). Both plus and minus polarities of sRNAs were
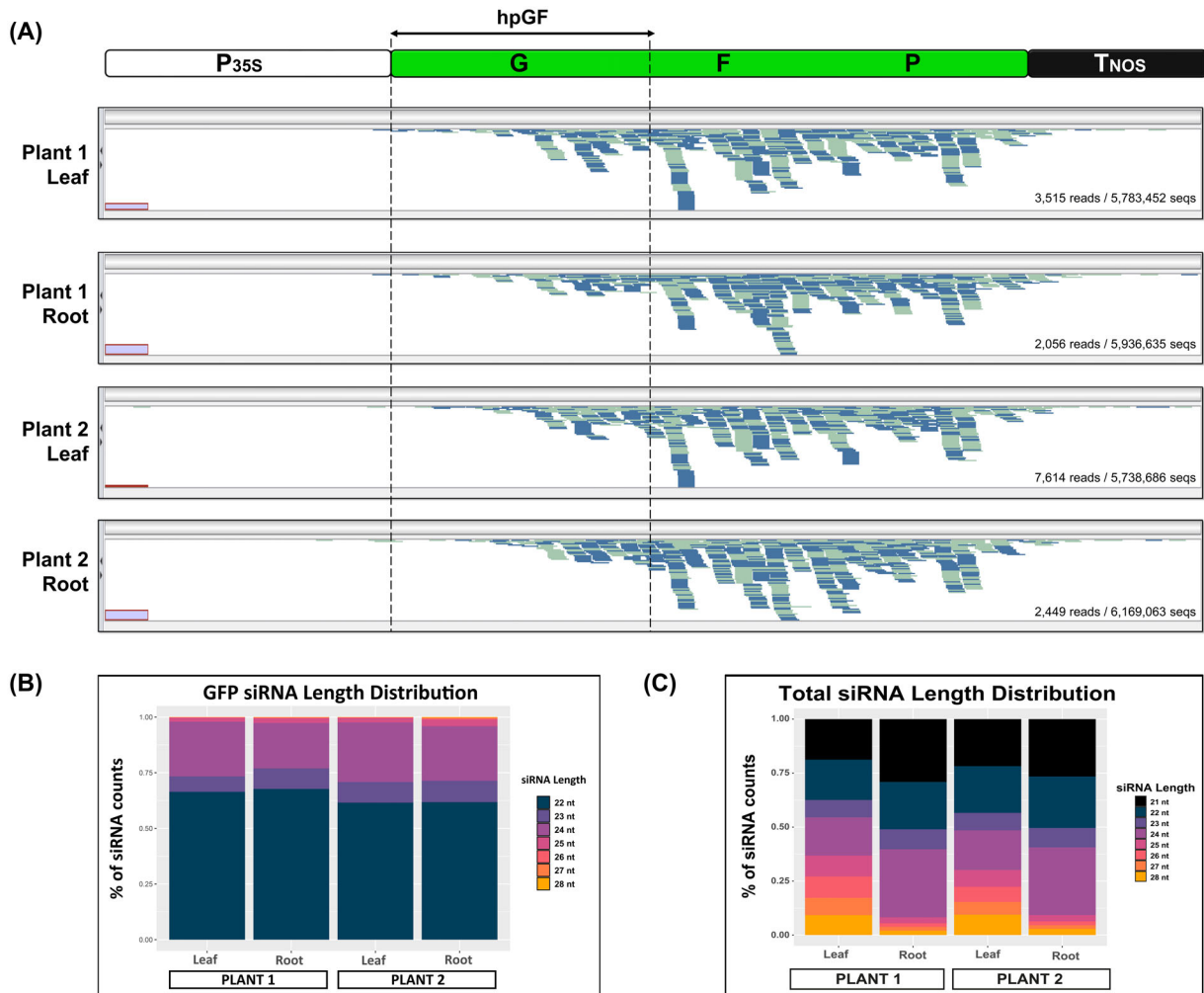
Fig. 2. sRNA seq in Nb-GFP16C fully silenced plants. Results are depicted for one out of two technical replicates for each tissue. (A) Depiction of all siRNA reads (22–30 nt) mapping to GFP region. siRNAs of plus polarity are depicted in light blue, and siRNAs of minus polarity are depicted in light green. siRNA reads were visualized using Tablet software (Milne *et al.* 2013). (B) Stacked bar chart representing the length distribution (22–28-nt) of sRNAs mapping to GFP sequence. (C) Stacked bar chart representing the length distribution (21–28-nt) of total sRNAs mapping to the host genome.

detected (Fig. 2A). Interestingly, sRNAs were more abundant in the P region rather than in the GF region (Fig. 2A). This is noteworthy, since P sRNAs only reflect obligatory RDR6-produced secondary sRNAs. It is not clear which portion of the detected GF sRNAs are primary fungal sRNAs that were translocated from the hyphae to the root and possibly transported systemically throughout the plant, and which of them were secondarily produced by RDRs. Since, although we have not observed any differences among the fungus-enriched root tissues and the leaf tissues, we can assume that the population of primary fungal GF sRNAs was meagre and the majority of detected GF sRNAs represent host-derived secondary sRNAs.

An intriguing observation was made as regards the size distribution of the sRNAs mapping to *GFP*: in both root and leaf, the majority of sRNAs was 22-nt (60%), followed by 24-nt (25%), and 23-nt (10%) (Fig. 2B), while no 21-nt sRNA reads could be recorded. This absence does not reflect a sequencing technical error or a malfunction in the generation of 21-nt

sRNAs in the host upon FsK colonization, since our sRNA seq analysis revealed the abundant presence of 21-nt sRNAs mapping to the host genome and corresponding to endogenous miRNAs and other regulatory sRNAs, with the exclusion of *GFP* alone (Fig. 2C and Figure S2). This is the first time, to the best of our knowledge, that absence of 21-nt siRNAs is observed in transitivity studies. Previous reports have shown that RDR6-generated dsRNAs are processed mainly to 21 >22-nt sRNAs (Parent *et al.* 2015; Taochy *et al.* 2017; Wu *et al.* 2017; Uslu *et al.* 2020). In *N. benthamiana* DCL2 is more highly expressed than DCL4 (Nakasugi *et al.* 2013) and this likely accounts for the fact that, in some cases, RDR6-generated dsRNAs may be processed to 22 >21-nt sRNAs (Dalakouras *et al.* 2019). But the complete absence of 21-nt sRNAs was an unexpected outcome. The reasons for this observation still elude us. Yet, it should be noted that, in contrast to conventional RNAi induction systems so far (i.e., dsRNA-expressing transgenic plants, agroinfiltration of dsRNA constructs, virus-induced gene silencing, sprayed sRNAs) that generate sufficient
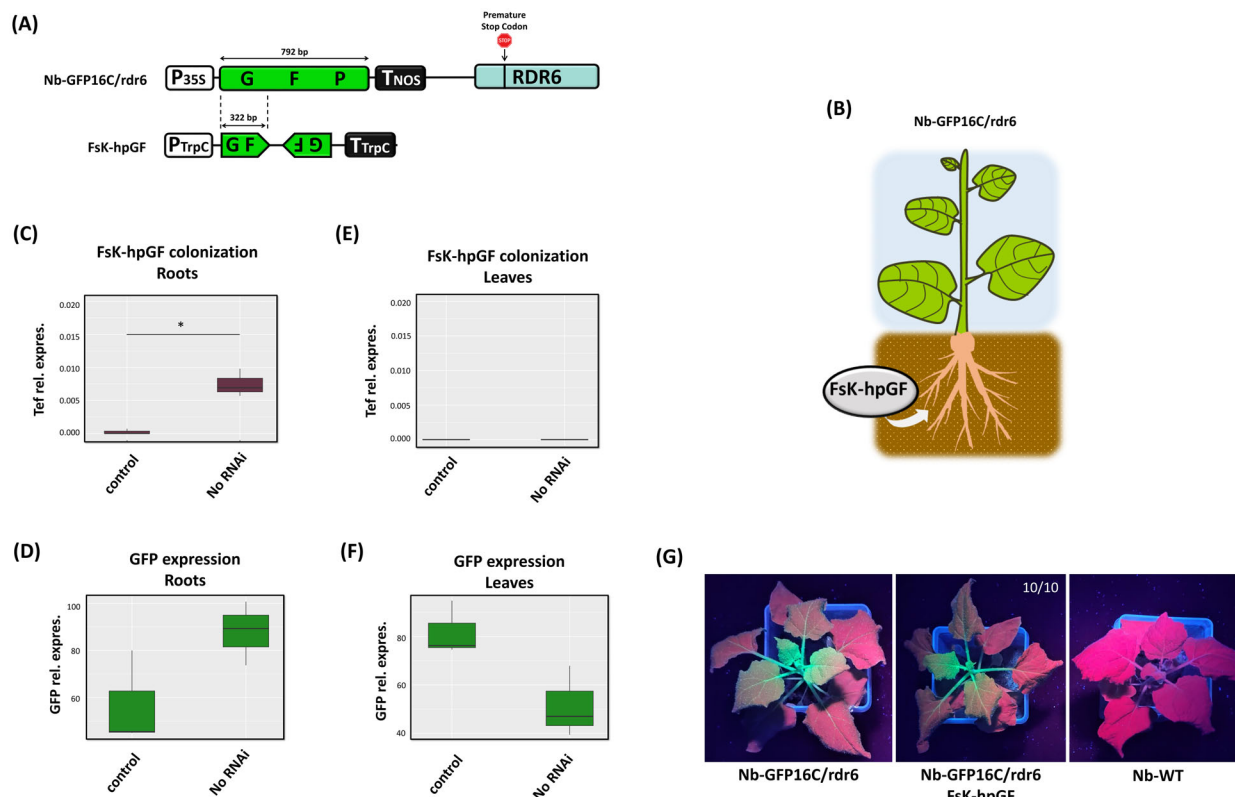
Fig. 3. FsK hpGF colonization of Nb-GFP16C/rdr6 plants. (A) Schematic representation of Nb-GFP16C/rdr6 plants, where the non-functional RDR6 is depicted (stop codon). (B) Schematic overview of the colonization assay. (C) RT-qPCR for estimation of fungal colonization levels (*Tef* gene) in roots of the Nb-GFP16C/rdr6 plants at 9 wpi. Expression levels are normalized to the Nb *Act* gene, each category represented by three biological replicates (n = 3), with all samples run in two technical replicates. A *t*-test showed statistical significance (*P*-value <0.05). (D) RT-qPCR for the estimation of *gfp* mRNA expression in roots of the plants at 9 wpi. Expression levels are normalized to *N. benthamiana Act* gene, each category represented by three biological replicates (n = 3), with all samples run in two technical replicates. A *t*-test showed no statistical significance (*P*-value >0.05). (E) RT-qPCR for estimation of fungal colonization levels (*Tef* gene) in leaves of the Nb-GFP16C/rdr6 plants at 9 wpi. Expression levels are normalized to the Nb *Act* gene, each category represented by three biological replicates (n = 3), with all samples run in two technical replicates. (F) RT-qPCR for estimation of *GFP* mRNA expression in leaves of the plants at 9 wpi. Expression levels are normalized to the Nb *Act* gene, each category represented by three biological replicates (n = 3), with all samples run in two technical replicates. A *t*-test showed no statistical significance (p-value >0.05). (G) Representative pictures of non-colonized versus FsK-hpGF-colonized Nb-GFP16C/rdr6 plants (in total 10 plants were studied from each category) under ultraviolet light at 7 wpi. The Nb-WT plant was used as a phenotypic control of chlorophyll fluorescence. No silencing phenotype was detected.

quantities of primary sRNAs, our system was likely initiated by negligible amounts of primary (fungal) sRNAs that relied on RDR6-based amplification in order to surpass a threshold and establish RNAi. Nevertheless, the fact that the silenced tissue lacked 21-nt sRNAs, suggests that the species responsible for GFP mRNA degradation were 22-nt sRNAs, confirming that 22-nt sRNAs may not only recruit RDR6 (Mlotshwa *et al*. 2008; Chen *et al*. 2010; Dalakouras *et al*. 2016b; Hendrix *et al*. 2021) or block translation (Wu *et al*. 2020), but also mediate mRNA cleavage.

FsK failed to trigger RNAi in *rdr6* knockout background

To further demonstrate that the fungal primary sRNAs fail or are not sufficient to establish RNAi in the host, and that RDR6-based amplification of sRNA pool is required, we resolved to a genetic approach and used the Nb-GFP16C homozygous for CRISPR/Cas-edited *RDR6* mutant plant line (Nb-GFP16C/rdr6). This line contains a single insertion of T leading to a frame shift and premature stop codon in the *RDR6*

reading frame (Ludman & Fátyol 2019), and was crossed with the Nb-GFP16C homozygous line (Ebrahimi *et al*. 2023). We inoculated Nb-GFP16C/rdr6 with FsK-hpGF and repeated the same procedures for recording systemic silencing, as described above for the Nb-GFP16C line (Fig. 3A,B). We first verified that indeed Fsk-hpGF colonized again only the root but not the aerial part of the plant (Fig. 3C,E), as observed in Nb-GFP16C. Phenotypic analysis under UV light (Fig. 3G) and RT-qPCR revealed the absence of silencing in both tissues (Fig. 3D,F) even after 9 weeks post-inoculation. In this view, our observations further support the hypothesis that the primary fungal GF sRNAs alone are not sufficient to trigger efficient RNAi in the host; only when transitivity occurs, is widespread systemic silencing established.

FsK failed to trigger RNAi to a host intron-containing gene

To further assess and verify the importance of RDR6-produced secondary sRNAs in the establishment of RNAi in the host plant by the root endophyte, we inoculated FsK-hpGF to a
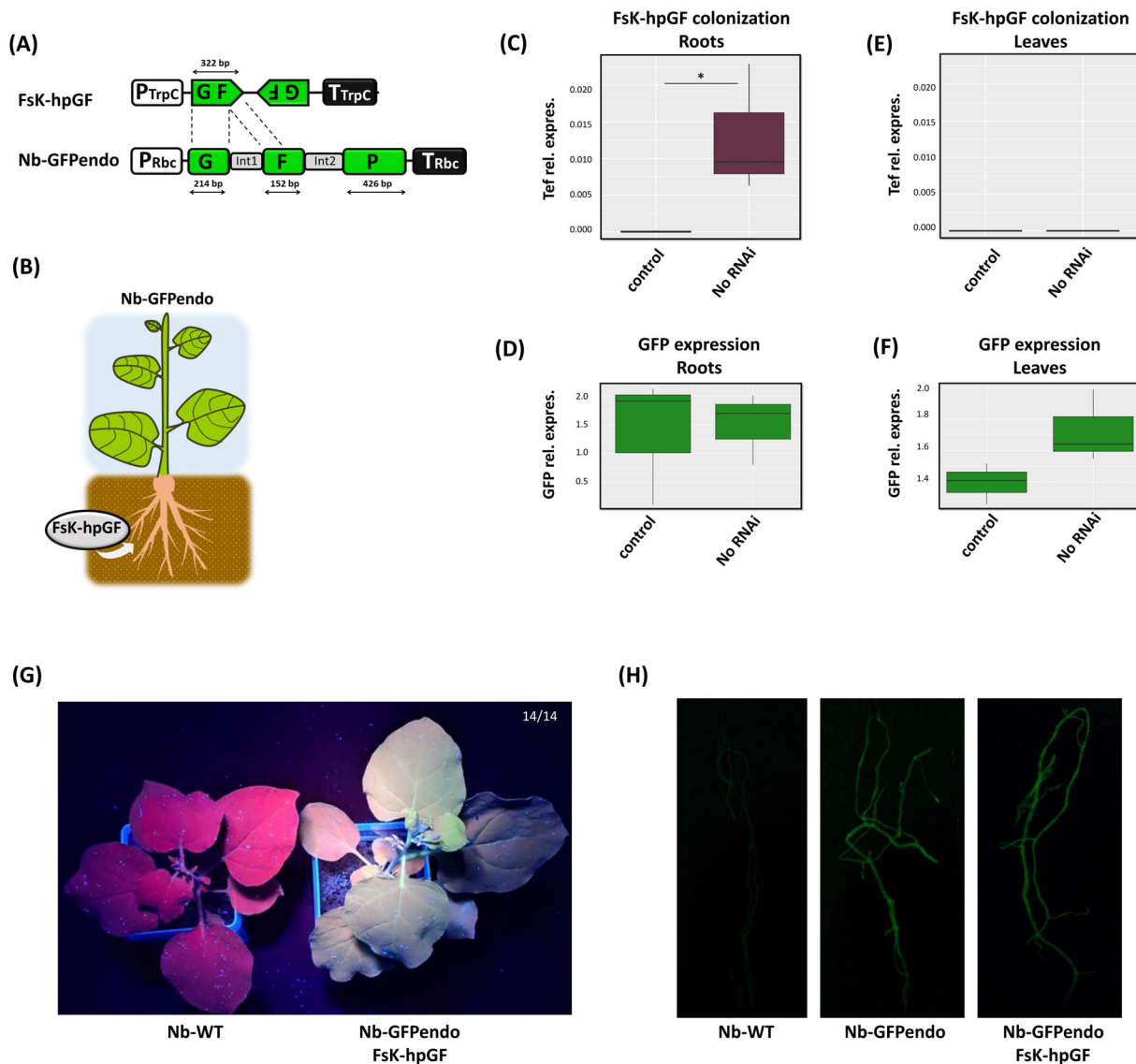
Fig. 4. FsK hpGF colonization of Nb-GFPendo plants. (A) Schematic representation of the *GFP* transgene present in the hpGF construct of FsK and Nb-GFPendo line. PTrpC promoter from *Aspergillus nidulans trpC* gene; GF: 322 bp fragment of *GFP*; TTrpC: terminator from *Aspergillus nidulans trpC* gene; GFP: full-length (792 bp) green fluorescent protein (*mGFP-ER* version), PRbc: tobacco *RuBisCO* small subunit promoter including 5'UTR; G:214 bp fragment of *GFP*; Int1:intron 1 genetic element of *RuBisCO* small subunit; F:152 bp fragment of *GFP*; Int2: intron 2 genetic element of *RuBisCO* small subunit; P: 426 bp fragment of *GFP*; TRbc: tobacco *RuBisCO* small subunit terminator including 3'UTR. (B) Schematic overview of the colonization assay. (C) RT-qPCR for estimation of fungal colonization levels (*Tef* gene) in roots of the Nb-GFPendo plants at 9 wpi. Expression levels are normalized to the Nb *Act* gene, each category represented by three biological replicates (n = 3), with all samples run in two technical replicates. A *t*-test showed statistical significance (p-value <0.05). (D) RT-qPCR for estimation of *GFP* mRNA expression in roots of the plants at 9 wpi. Expression levels are normalized to the Nb *Act* gene, each category represented by three biological replicates (n = 3), with all samples run in two technical replicates. A *t*-test showed no statistical significance (*P*-value >0.05). (E) RT-qPCR for estimation of fungal colonization levels (*Tef* gene) in leaves of the Nb-GFPendo plants at 9 wpi. Expression levels are normalized to the Nb *Act* gene, each category represented by three biological replicates (n = 3), with all samples run in two technical replicates. (F) RT-qPCR for estimation of *GFP* mRNA expression in leaves of the plants at 9 wpi. Expression levels are normalized to the Nb *Act* gene, each category represented by three biological replicates (n = 3), with all samples run in two technical replicates. A *t*-test showed no statistical significance (*P*-value >0.05). (G) Representative picture of a colonized Nb-GFPendo plant (in total 14 plants were studied) under ultraviolet light at 5 wpi, Nb-WT plant is used as a phenotypic control for chlorophyll fluorescence. (H) Stereoscopic observation of GFP fluorescence in roots of non-colonized versus hpGF colonized Nb-GFPendo plants at 9 wpi. Nb-WT was used as negative control of root autofluorescence.

N. benthamiana plant line carrying an endogene-like *GFP* transgene, namely Nb-GFPendo. In contrast to Nb-GFP16C that harbours an intronless *GFP* cDNA unit under the control of *35S* promoter and *NOS* terminator, the *GFP* transgene in Nb-GFPendo was designed to resemble the structure of the highly transcribed small subunit of *RIBULOSE-1,5-BISPHOSPHATE CARBOXYLASE-OXYGENASE* (*RuBisCO*) gene, consisting of *RuBisCO* promoter and terminator in
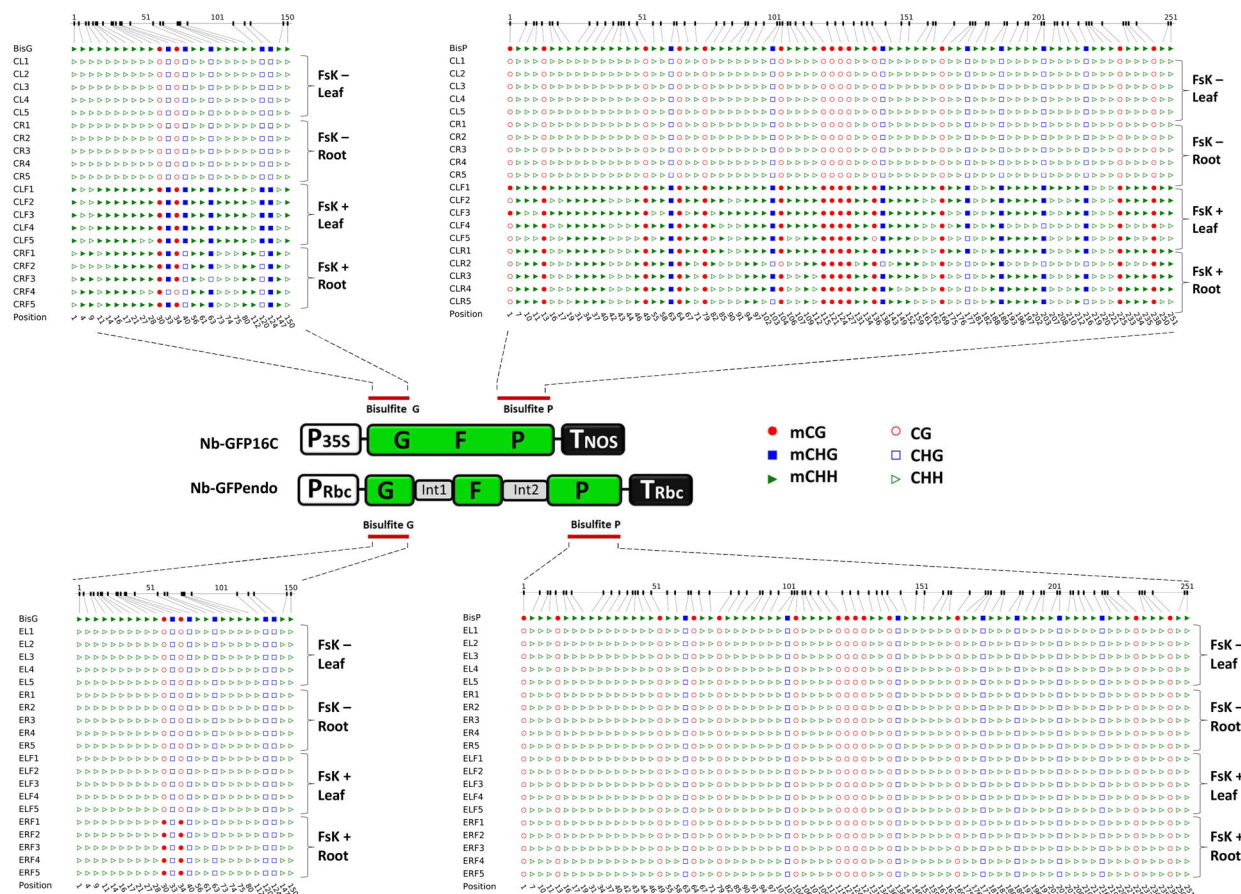
Fig. 5. Bisulfite sequencing of host GFP in both roots and leaves of Nb-GFP16C and Nb-GFPendo plants. Two regions of the *GFP* sequence were analysed; Bisulfite G and Bisulfite P. Results are visualized with CyMATE software (Hetzl *et al.* 2007). Each shape represents cytosine residues in different sequence contexts; CG as red circles, CHG as blue rectangles and CHH as green triangles. Empty symbols refer to nonmethylated cytosines, whereas filled symbols refer to methylated cytosines.

addition to two *RuBisCO* introns that separated arbitrarily three *GFP* exons (Fig. 4A) (Dadami *et al.* 2013, 2014). It is well-established that aberrant RNAs (abRNAs) occurring from intron-containing genes seem to be degraded via the exonucleolytic RNA decay pathway and not by the RDR6/RNAi pathway, and the presence of introns and spliceosome association to the pre-mRNA also seems to inhibit RDR6 (Christie *et al.* 2011; Christie & Carroll 2011). Indeed, genome-wide analyses of *Arabidopsis* sRNA libraries showed that exons from intron-containing genes accumulate less sRNAs than exons from intronless genes. In *Arabidopsis*, it has been proposed that the interaction of spliceosome with ABA HYPESENSI-TIVE 1 (ABH1), a human CA-binding protein 80 ortholog and SERRATE (SE), a zinc finger protein known to function in miRNA biogenesis, inhibits RDR6 recruitment (Christie & Carroll 2011). Such a mechanism could reflect a mechanism adapted through evolution by plants to target 'non-self' viral genes rather than 'self' intron-containing genes. Thus, intron-containing transgenes under the control of a strong promoter generate few, if any, abRNAs that can be processed by RDR6. Thus, we reasoned that, in contrast to Nb-GFP16C, the Nb-GFPendo plant line would not generate transcripts that could be processed by RDR6 or generate very few of them, below a certain threshold level that likely seems

to be exceeded for the establishment of RNAi (Kalantidis *et al.* 2006, 2008). Indeed, our observations validated our hypothesis. As in Nb-GFP16C and Nb-GFP16C/rdr6, FsK-hpGF colonized the root but not the aerial part of Nb-GFPendo (Fig. 4B,C,E). But contrary to the Nb-GFP16C, there were no signs of RNAi in Nb-GFPendo roots or leaves neither upon RT-qPCR analysis (Fig. 4D,F) nor under GFP visualization (Fig. 4G,H). There is no reason to assume that FsK-hpGF does not translocate sRNAs to Nb-GFPendo, since it translocates them to Nb-GFP16C. Indeed, we assume that few amounts of fungal primary GF sRNAs are similarly present in both Nb-GFP16C and Nb-GFPendo. However, in contrast to Nb-GFP16C, where RDR6-based amplification of silencing signals occurs, no such amplification occurs in Nb-GFPendo for the reasons explained above. These results further support the central role of RDR6 and corroborate that transitivity is required in establishing widespread systemic silencing in the host.

FsK triggers RdDM to a host intronless but not to an intron-containing gene

Induction of PTGS in plants is tightly coupled to RdDM of the corresponding coding region (Jones *et al.* 2001). Moreover,
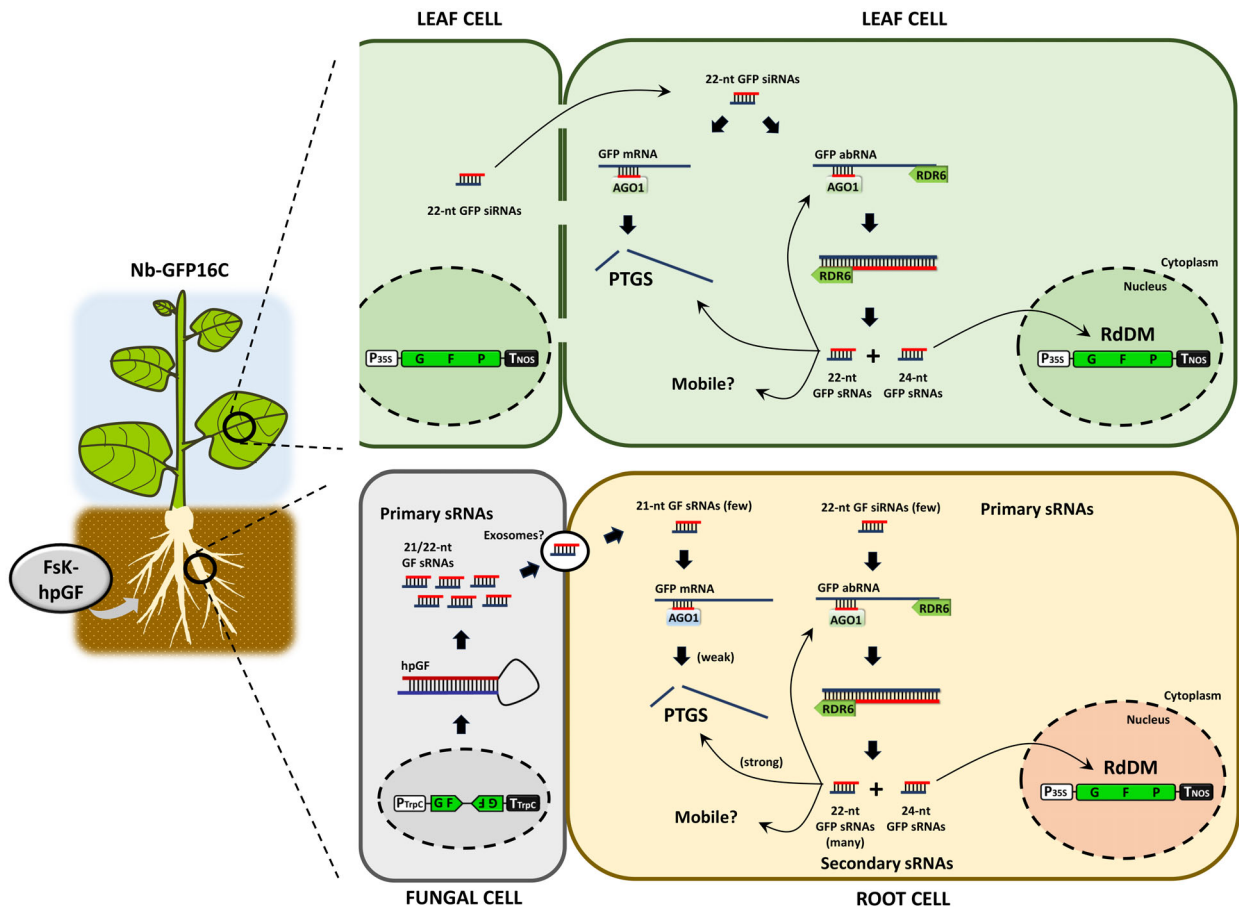
Fig. 6. Proposed mechanism of our RNAi system in Nb-GFP16C plants. FsK colonizes the root system of the plant. Inside the fungal cell, hpGF is transcribed and cleaved by FsK's DCLs into primary GF siRNAs (21 and 22 nt long). These GF siRNAs (and/or even the GF hairpin itself) travel to the plant root cells through an unknown mechanism (probably through exosomes and clathrin-mediated endocytosis). Inside the root cells the few 21-nt fungal GF siRNAs trigger degradation of the plant GFP, causing weak PTGS. The 22-nt fungal GF siRNAs recruit RDR6, leading to amplification of the initial RNAi signal and production of secondary 22-nt and 24-nt long siRNAs. The 24-nt siRNAs trigger methylation of complementary DNA in the nucleus, while the 22-nt trigger further PTGS but also are transported to the upper part of the plant. In the upper plant part, secondary siRNAs move from leaf to leaf through the plasmodesmata, triggering PTGS and also further amplification of silencing.

RDR6 is dispensable for the establishment of coding region RdDM upon PTGS (Vaistij & Jones 2009). Since a fraction of the RDR6-generated secondary sRNAs in FsK-hpGF-colonized Nb-GFP16C were of 24-nt in size (Fig. 2B), known to be involved in the RdDM pathway (Chan *et al.* 2004), we examined the DNA methylation status of the *GFP* coding region in both root and leaf tissues of the systemically silenced Nb-GFP16C plants. Indeed, bisulfite sequencing revealed the establishment of dense RdDM patterns in both GF and P regions and in both root and leaf tissues in every sequence context (CG, CHG, CHH) (Fig. 5). CHH methylation is the hallmark of ongoing *de novo* RdDM (Pelissier *et al.* 1999) and is in full agreement with the ongoing RNAi taking place at the tissue of analysis. In contrast, in the FsK-hpGF-colonized Nb-GFPendo plants that showed no signs of silencing, bisulfite sequencing analysis of the same regions that were analysed in Nb-GFP16C plants revealed the absence of cytosine methylation in both roots and leaves, with the exception of few methylated cytosines at CG context in the root tissue and only in the GF region (Fig. 5). It is not clear whether the few primary fungal GF sRNAs are accountable for this negligible methylation event.

Overall, these data underpin that epigenetic changes may occur during mutualistic interactions, especially when these are accompanied by systemic silencing phenomena. Supporting our observations, epigenetic reprogramming has been shown to take place in *Arabidopsis* colonized with *Trichoderma atroviride* (Rebolledo-Prudencio *et al.* 2021) and polar trees with *Laccaria bicolor* (Vigneaud *et al.* 2023). Whether such epigenetic modifications are trans-generationally maintained even in the absence of colonization has not been investigated yet.

CONCLUSION

This report reinforces a growing body of evidence showing that beneficial fungal endophytes may impose their impacts by translocating RNAi molecules to modulate host gene expression (Secic *et al.* 2021; Wong-Bajracharya *et al.* 2022). Yet, the data presented here reveal that RDR6-mediated amplification of RNAi signals is indispensable for overcoming a certain threshold level that leads to meaningful and widespread RNAi (Fig. 6). Moreover, our data suggest that intronless endogenous genes may be better candidates for such a mode of action, rather than

intron-containing genes. Future studies aiming to identify endogenous host targets of endogenous fungal sRNAs that could be accountable for the imposing of the beneficial phenotype may thus need to pay special attention to intronless candidates. The fact that not only mRNA degradation but also DNA methylation is involved in the whole process of fungus-induced host silencing underpins that establishment of mutualistic associations between fungi and their host could also be based on epigenetic reprogramming (Rebolledo-Prudencio *et al.* 2021; Vigneaud *et al.* 2023). Importantly, our data suggest that the indispensable role of RDR6 in the establishment of systemic silencing phenotypes may not be restricted to symbionts but also to pathogens, although this hypothesis remains to be validated.

AUTHOR CONTRIBUTIONS

KPP and AD concieved the idea and supervised research. LMK, AD and PV carried out the experiments. OT contributed to the bioinformatic analysis and VVU with resources. LMK led the data acquisition and analysis. LMK, AD and KKP wrote the manuscript. All authors edited the manuscript and approved the final version.

ACKNOWLEDGEMENTS

SUPPORTING INFORMATION

Additional supporting information may be found online in the Supporting Information section at the end of the article.

Figure S1. RT-qPCR for estimation of fungal colonization levels in the root system of systemic silenced Nb-GFP16C plants at 9 wpi. Samples are categorized by inoculation concentration (10^2, 10^3, 10^4 conidia) and silencing phenotype (No RNA, RNAi spots, RNAi veins, RNAi full). The whole root system of a plant in each silencing phenotype was used to estimate expression levels of the *Tef* gene normalized to the Nb *Act* gene. All samples were run in two technical replicates.

Figure S2. Detection of selected Nb miRNAs (miR159, miR166, miR396, and miR403) having a size of 21-nt in FsK-hpGF-colonized Nb-GFP16C plants.

Table S1. Sequences of all primers used in this study.

REFERENCES

Anders S., Pyl P.T., Huber W. (2014) HTSeq—A python framework to work with high-throughput sequencing data. *Bioinformatics*, **31**, 166–169.

Baksa I., Nagy T., Barta E., Havelda Z., Várallyay É., Silhavy D., Burgyán J., Szittya G. (2015) Identification of *Nicotiana benthamiana* microRNAs and their targets using high throughput sequencing and degradome analysis. *BMC Genomics*, **16**, 1025.

Cai Q., Halilovic L., Shi T., Chen A., He B., Wu H., Jin H. (2023) Extracellular vesicles: Cross-organismal RNA trafficking in plants, microbes, and mammalian cells. *Extracellular Vesicles and Circulating Nucleic Acids*, **4**, 262–282.

Cai Q., Qiao L., Wang M., He B., Lin F.M., Palmquist J., Huang S.D., Jin H. (2018) Plants send small RNAs in extracellular vesicles to fungal pathogen to silence virulence genes. *Science*, **360**, 1126–1129.

Cao X., Aufsatz W., Zilberman D., Mette M.F., Huang M.S., Matzke M., Jacobsen S.E. (2003) Role of the DRM and CMT3 methyltransferases in RNA-directed DNA methylation. *Current Biology*, **13**, 2212–2217.

Chan S.W., Zilberman D., Xie Z., Johansen L.K., Carrington J.C., Jacobsen S.E. (2004) RNA silencing genes control de novo DNA methylation. *Science*, **303**, 1336.

Chen H.M., Chen L.T., Patel K., Li Y.H., Baulcombe D.C., Wu S.H. (2010) 22-nucleotide RNAs trigger secondary siRNA biogenesis in plants. *Proceedings of the National Academy of Sciences*, **107**, 15269–15274.

Cheng A.P., Kwon S., Adeshara T., Göhre V., Feldbrügge M., Weiberg A. (2023) Extracellular RNAs released by plant-associated fungi: From fundamental mechanisms to biotechnological applications. *Applied Microbiology and Biotechnology*, **107**, 5935–5945. https://doi.org/10.1007/s00253-023-12718-7

Christie M., Carroll B.J. (2011) SERRATE is required for intron suppression of RNA silencing in Arabidopsis. *Plant Signaing andl Behavior*, **6**, 2035–2037. https://doi.org/10.4161/psb.6.12.18238

Christie M., Croft L.J., Carroll B.J. (2011) Intron splicing suppresses RNA silencing in Arabidopsis. *The Plant Journal*, **68**, 159–167.

Dadami E., Dalakouras A., Zwiebel M., Krczal G., Wassenegger M. (2014) An endogene-resembling transgene is resistant to DNA methylation and systemic silencing. *RNA Biology*, **11**, 934–941.

Dadami E., Moser M., Zwiebel M., Krczal G., Wassenegger M., Dalakouras A. (2013) An endogene-resembling transgene delays the onset of silencing and limits siRNA accumulation. *FEBS Letters*, **587**, 706–710.

Dalakouras A., Dadami E., Wassenegger M., Krczal G., Wassenegger M. (2016a) RNA-directed DNA methylation efficiency depends on trigger and target sequence identity. *The Plant Journal*, **87**, 202–214.

Dalakouras A., Katsaouni A., Avramidou M., Dadami E., Tsiouri O., Vasileiadis S., Makris A., Georgopoulou M.E., Papadopoulou K.K. (2023) A beneficial fungal root endophyte triggers systemic RNA silencing and DNA methylation of a host reporter gene. *RNA Biology*, **20**, 20–30.

Dalakouras A., Lauter A., Bassler A., Krczal G., Wassenegger M. (2019) Transient expression of intron-containing transgenes generates non-spliced aberrant pre-mRNAs that are processed into siRNAs. *Planta*, **249**, 457–468.

Dalakouras A., Wassenegger M., McMillan J.N., Cardoza V., Maegele I., Dadami E., Runne M., Krczal G., Wassenegger M. (2016b) Induction of silencing in plants by high-pressure spraying of in vitro-synthesized small RNAs. *Frontiers in Plant Science*, **7**, 1327. https://doi.org/10.3389/fpls.2016.01327/abstract

Dalmay T., Hamilton A., Rudd S., Angell S., Baulcombe D.C. (2000) An RNA-dependent RNA polymerase gene in Arabidopsis is required for posttranscriptional gene silencing mediated by a transgene but not by a virus. *Cell*, **101**, 543–553.

de Felippes F.F., Waterhouse P.M. (2020) The whys and wherefores of transitivity in plants. *Frontiers in Plant Science*, **11**, 579376. https://doi.org/10.3389/fpls.2020.579376

Devers E.A., Brosnan C.A., Sarazin A., Schott G., Lim P., Lehesranta S., Helariutta Y., Voinnet O. (2023) In planta dynamics, transport biases, and endogenous functions of mobile siRNAs in Arabidopsis. *The Plant Journal.*, **115**, 1377–1393.

Ebrahimi S., Eini O., Baßler A., Hanke A., Yildirim Z., Wassenegger M., Krczal G., Uslu V.V. (2023) Beet curly top Iran virus rep and V2 suppress posttranscriptional gene silencing via distinct modes of action. *Viruses*, **15**, 1996. https://doi.org/10.3390/v15101996

Ewels P., Magnusson M., Lundin S., Käller M. (2016) MultiQC: Summarize analysis results for multiple tools and samples in a single report. *Bioinformatics*, **32**, 3047–3048.

Fernandez-Pozo N., Menda N., Edwards J.D., Saha S., Tecle I.Y., Strickler S.R., Bombarely A., Fisher-York T., Pujar A., Foerster H., Yan A., Mueller L.A. (2015) The sol genomics network (SGN)--from genotype to phenotype to breeding. *Nucleic Acids Research*, **43**, D1036–D1041.

Hamilton A.J., Baulcombe D.C. (1999) A species of small antisense RNA in posttranscriptional gene silencing in plants. *Science*, **286**, 950–952.

513

He B., Hamby R., Jin H. (2021) Plant extracellular vesicles: Trojan horses of cross-kingdom warfare. *FASEB Bioadvances*, **3**, 657–664.

Henderson I.R., Zhang X., Lu C., Johnson L., Meyers B.C., Green P.J., Jacobsen S.E. (2006) Dissecting Arabidopsis thaliana DICER function in small RNA processing, gene silencing and DNA methylation patterning. *Nature Genetics*, **38**, 721–725.

Hendrix B., Zheng W., Bauer M.J., Havecker E.R., Mai J.T., Hoffer P.H., Sanders R.A., Eads B.D., Caruano-Yzermans A., Taylor D.N., Hresko C., Oakes J., Iandolino A.B., Bennett M.J., Deikman J. (2021) Topically delivered 22 nt siRNAs enhance RNAi silencing of endogenous genes in two species. *Planta*, **254**, 60.

Hetzl J., Foerster A.M., Raidl G., Mittelsten Scheid O. (2007) CyMATE: A new tool for methylation analysis of plant genomic DNA after bisulphite sequencing. *The Plant Journal*, **51**, 526–536.

Jiao J., Peng D. (2018) Wheat microRNA1023 suppresses invasion of *fusarium graminearum* via targeting and silencing FGSG_03101. *Journal of Plant Interactions*, **13**, 514–521.

Jones L., Ratcliff F., Baulcombe D.C. (2001) RNA-directed transcriptional gene silencing in plants can be inherited independently of the RNA trigger and requires Met1 for maintenance. *Current Biology*, **11**, 747–757.

Kalantidis K., Schumacher H.T., Alexiadis T., Helm J.M. (2008) RNA silencing movement in plants. *Biology of the Cell*, **100**, 13–26.

Kalantidis K., Tsagris M., Tabler M. (2006) Spontaneous short-range silencing of a GFP transgene in *Nicotiana benthamiana* is possibly mediated by small quantities of siRNA that do not trigger systemic silencing. *The Plant Journal*, **45**, 1006–1016.

Kavroulakis N., Ntougias S., Zervakis G.I., Ehaliotis C., Haralampidis K., Papadopoulou K.K. (2007) Role of ethylene in the protection of tomato plants against soil-borne fungal pathogens conferred by an endophytic fusarium solani strain. *Journal of Experimental Botany*, **58**, 3853–3864.

Langmead B., Salzberg S.L. (2012) Fast gapped-read alignment with bowtie 2. *Nature Methods*, **9**, 357–359.

Langmead B., Trapnell C., Pop M., Salzberg S.L. (2009) Ultrafast and memory-efficient alignment of short DNA sequences to the human genome. *Genome Biology*, **10**, R25.

Leichter S.M., Du J., Zhong X. (2022) Structure and mechanism of plant DNA methyltransferases. *Advances in Experimental Medicine and Biology*, **1389**, 137–157.

Livak K.J., Schmittgen T.D. (2001) Analysis of relative gene expression data using real-time quantitative PCR and the 2(-Delta Delta C(T)) method. *Methods*, **25**, 402–408. https://doi.org/10.1006/meth.2001.1262

Ludman M., Fátyol K. (2019) The virological model plant, Nicotiana benthamiana expresses a single functional RDR6 homeolog. *Virology*, **537**, 143–148.

Martin M. (2011) CUTADAPT removes adapter sequences from high-throughput sequencing reads. *EMBnet.journal*, **17**, 10. https://doi.org/10.14806/ej.17.1.200

Milne I., Stephen G., Bayer M., Cock P.J., Pritchard L., Cardle L., Shaw P.D., Marshall D. (2013) Using tablet for visual exploration of second-generation sequencing data. *Briefings in Bioinformatics*, **14**, 193–202.

Mlotshwa S., Pruss G.J., Peragine A., Endres M.W., Li J., Chen X., Poethig R.S., Bowman L.H., Vance V. (2008) DICER-LIKE2 plays a primary role in transitive silencing of transgenes in Arabidopsis. *PLoS One*, **3**, e1755.

Nakasugi K., Crowhurst R.N., Bally J., Wood C.C., Hellens R.P., Waterhouse P.M. (2013) De novo transcriptome sequence assembly and analysis of RNA silencing genes of Nicotiana benthamiana. *PLoS One*, **8**, e59534.

Parent J.-S., Bouteiller N., Elmayan T., Vaucheret H. (2015) Respective contributions of Arabidopsis DCL2 and DCL4 to RNA silencing. *The Plant Journal*, **81**, 223–232.

Pelissier T., Thalmeir S., Kempe D., Sanger H.L., Wassenegger M. (1999) Heavy de novo methylation at symmetrical and non-symmetrical sites is a hallmark of RNA-directed DNA methylation. *Nucleic Acids Research*, **27**, 1625–1634.

Rebolledo-Prudencio O.G., Estrada-Rivera M., Dautt-Castro M., Arteaga-Vazquez M.A., Arenas-Huertero C., Rosendo-Vargas M.M., Jin H., Casas-Flores S. (2021) The small RNA-mediated gene silencing machinery is required in Arabidopsis for stimulation of growth, systemic disease resistance, and suppression of the nitrile-specifier gene NSP4 by Trichoderma atroviride. *The Plant Journal*, **109**, 873–890. https://doi.org/10.1111/tpj.15599

Reinhart B.J., Weinstein E.G., Rhoades M.W., Bartel B., Bartel D.P. (2002) MicroRNAs in plants. *Genes and Development*, **16**, 1616–1626.

Secic E., Zanini S., Wibberg D., Jelonek L., Busche T., Kalinowski J., Nasfi S., Thielmann J., Imani J., Steinbrenner J., Kogel K.H. (2021) A novel plant-fungal association reveals fundamental sRNA and gene expression reprogramming at the onset of symbiosis. *BMC Biology*, **19**, 171.

Silvestri A., Fiorilli V., Miozzi L., Accotto G.P., Turina M., Lanfranco L. (2019) In silico analysis of fungal sRNA accumulation reveals putative plant mRNA targets in the symbiosis between an arbuscular mycorrhizal fungus and its host plant. *BMC Genomics*, **20**, 169.

Skiada V., Avramidou M., Bonfante P., Genre A., Papadopoulou K.K. (2020) An endophytic fusarium–legume association is partially dependent on the common symbiotic signalling pathway. *New Phytologist*, **226**, 1429–1444.

Taochy C., Gursanscky N.R., Cao J., Fletcher S.J., Dressel U., Mitter N., Tucker M.R., Koltunow A.M.G., Bowman J.L., Vaucheret H., Carroll B.J. (2017) A genetic screen for impaired systemic RNAi highlights the crucial role of DICER-LIKE 2. *Plant Physiology*, **175**, 1424–1437.

Uslu V.V., Bassler A., Krczal G., Wassenegger M. (2020) High-pressure-sprayed double stranded RNA does not induce RNA interference of a reporter gene. *Frontiers in Plant Science*, **11**, 534391.

Vaistij F.E., Jones L. (2009) Compromised virus-induced gene silencing in RDR6-deficient plants. *Plant Physiology*, **149**, 1399–1407. https://doi.org/10.1104/pp.108.132688

Vaucheret H., Voinnet O. (2024) The plant siRNA landscape. *The Plant Cell*, **36**, 246–275.

Vigneaud J., Kohler A., Sow M.D., Delaunay A., Fauchery L., Guinet F., Daviaud C., Barry K.W., Keymanesh K., Johnson J., Singan V., Grigoriev I., Fichot R., Conde D., Perales M., Tost J., Martin F.M., Allona I., Strauss S.H., Veneault-Fourrey C., Maury S. (2023) DNA hypomethylation of the host tree impairs interaction with mutualistic ectomycorrhizal fungus. *New Phytologist*, **238**, 2561–2577.

Voinnet O., Baulcombe D.C. (1997) Systemic signalling in gene silencing. *Nature*, **389**, 553.

Wang B., Sun Y., Song N., Zhao M., Liu R., Feng H., Wang X., Kang Z. (2017) Puccinia striiformis f. sp. tritici microRNA-like RNA 1 (Pst-milR1), an important pathogenicity factor of Pst, impairs wheat resistance to Pst by suppressing the wheat pathogenesis-related 2 gene. *New Phytologist*, **215**, 338–350.

Wang F., Huang H.Y., Huang J., Singh J., Pikaard C.S. (2023) Enzymatic reactions of AGO4 in RNA-directed DNA methylation: siRNA duplex loading, passenger strand elimination, target RNA slicing, and sliced target retention. *Genes & Development*, **37**, 103–118.

Wang M., Weiberg A., Lin F.M., Thomma B.P., Huang H.D., Jin H. (2016) Bidirectional cross-kingdom RNAi and fungal uptake of external RNAs confer plant protection. *Nature Plants*, **2**, 16151.

Wassenegger M., Dalakouras A. (2021) Viroids as a tool to study RNA-directed DNA methylation in plants. *Cells*, **10**, 1187.

Wassenegger M., Heimes S., Riedel L., Sanger H.L. (1994) RNA-directed de novo methylation of genomic sequences in plants. *Cell*, **76**, 567–576.

Weiberg A., Wang M., Lin F.M., Zhao H., Zhang Z., Kaloshian I., Huang H.D., Jin H. (2013) Fungal small RNAs suppress plant immunity by hijacking host RNA interference pathways. *Science*, **342**, 118–123.

Wen H.-G., Zhao J.-H., Zhang B.-S., Gao F., Wu X.-M., Yan Y.-S., Zhang J., Guo H.-S. (2023) Microbe-induced gene silencing boosts crop protection against soil-borne fungal pathogens. *Nature Plants*, **9**, 1409–1418. https://doi.org/10.1038/s41477-023-01507-9

Wong-Bajracharya J., Singan V.R., Monti R., Plett K.L., Ng V., Grigoriev I.V., Martin F.M., Anderson I.C., Plett J.M. (2022) The ectomycorrhizal fungus Pisolithus microcarpus encodes a microRNA involved in cross-kingdom gene silencing during symbiosis. *Proceedings of the National Academy of Sciences*, **119**, e2103527119.

Wu H., Li B., Iwakawa H.O., Pan Y., Tang X., Ling-Hu Q., Liu Y., Sheng S., Feng L., Zhang H., Zhang X., Tang Z., Xia X., Zhai J., Guo H. (2020) Plant 22-nt siRNAs mediate translational repression and stress adaptation. *Nature*, **581**, 89–93.

Wu Y.Y., Hou B.H., Lee W.C., Lu S.H., Yang C.J., Vaucheret H., Chen H.M. (2017) DCL2-and RDR6-dependent transitive silencing of SMXL4 and SMXL5 in Arabidopsis dcl4 mutants causes defective phloem transport and carbohydrate over-accumulation. *The Plant Journal*, **90**, 1064–1078.

Zand Karimi H., Baldrich P., Rutter B.D., Borniego L., Zajt K.K., Meyers B.C., Innes R.W. (2022) Arabidopsis apoplastic fluid contains sRNA- and circular RNA–protein complexes that are located outside extracellular vesicles. *The Plant Cell*, **34**, 1863–1881.

Zapletal D., Kubicek K., Svoboda P., Stefl R. (2023) Dicer structure and function: Conserved and evolving features. *EMBO Reports*, **24**, e57215.

Zhan J., Meyers B.C. (2023) Plant small RNAs: Their biogenesis, regulatory roles, and functions. *Annual Review of Plant Biology*, **74**, 21–51.

Zhang T., Zhao Y.L., Zhao J.H., Wang S., Jin Y., Chen Z.Q., Fang Y.Y., Hua C.L., Ding S.W., Guo H.S. (2016) Cotton plants export microRNAs to inhibit virulence gene expression in a fungal pathogen. *Nature Plants*, **2**, 16153.